

Seabed Morphology and Gas Venting Features in the Continental Slope Region of Krishna-Godavari Basin, Bay of Bengal: Implications in Gas-Hydrate Exploration

P. Dewangan^{1*}, T. Ramprasad¹, M. V. Ramana¹, A. Mazumdar¹, M. Desa¹, F. K. Badesab¹

¹National Institute of Oceanography (Council for Scientific and Industrial Research),
Dona Paula, Goa-403004, India

* for correspondence: pdewangan@nio.org, Scientist, National Institute of Oceanography, Donapaula, Goa-403004, India; Tel. No. +91-832-2450493; Fax. No. +91-832-2450609

Abstract

Increased oil and gas exploration activity has led to a detailed investigation of the continental shelf and adjacent slope regions of Mahanadi, Krishna-Godavari (KG) and Cauvery basins, which are promising petroliferous basins along the eastern continental margin of India. In this paper, we analyze the high resolution sparker, subbottom profiler and multibeam data in KG offshore basin to understand the shallow structures and shallow deposits for gas hydrate exploration. We identified and mapped prominent positive topographic features in the bathymetry data. These mounds show fluid/gas migration features such as acoustic voids, acoustic chimneys, and acoustic turbid layers. It is interesting to note that drilling/coring onboard JOIDES in the vicinity of the mounds show the presence of thick accumulation of subsurface gas hydrate. Further, geological and geochemical study of long sediment cores collected onboard Marion Dufresne in the vicinity of the mounds and sedimentary ridges shows the imprints of paleo-expulsion of methane and sulfidic fluid from the seafloor.

To understand the origin of the mounds and their relationship with gas hydrate/cold seep formation, we analyzed the multichannel seismic reflection (MCS) data close to the mounds. The MCS data show that the subsurface layers beneath the mounds are folded. Below the folded overburden, we observe zones of no coherent reflections probably originating from Miocene sequence. Since the study area is located in shale tectonics regime where Miocene sequences are known to be overpressured, we interpret the zones of no coherent reflections as Miocene shale diapirs. The upward movement of shale diapirs has folded the overburden layer and resulted in the formation of numerous faults/fractures. These faults act as permeable pathways for fluid/gas movement facilitating the formation of gas hydrate and cold seeps close to shale diapiric mound.

Keywords: shale tectonics; gas hydrates; BSR; echo facies; shale diapir; toe-thrust

1. Introduction

Offshore extension of the Krishna-Godavari (KG) basin is a proven petroliferous basin of eastern continental margin of India. The stratigraphy and tectonics of shelf and upper slope regions of the KG basin have been studied extensively for oil and gas exploration (Rao, 2001; Gupta, 2006; Singh and Swamy, 2006; Bastia, 2007). The pressure-temperature conditions in KG offshore basin (> 700 mbsf) is suitable for the formation of gas-hydrates, an ice-like crystalline solid in which methane and other lighter hydrocarbon gases are trapped inside the structure of water molecules (Sloan, 1990). The analysis of multi-channel seismic (MCS) data in KG offshore basin shows regional presence of gas hydrate manifested in the form of Bottom Simulating Reflectors (BSRs) (Ramana et al., 2007; Collett et al., 2008). Analysis of shallow sediment cores (~6 m) and shallow geophysical survey (Bathymetry, Chirp sonar and side scan sonar) shows evidences of pockmark, mud diapirism, slumping/sliding and other favorable indications for fluid/gas movements in KG offshore basin (Ramana et al., 2009). Analysis of long sediment core/logging data acquired onboard JOIDES Resolution (May-Aug., 2006) confirmed the presence of subsurface gas hydrate in KG offshore basin (Collett et al., 2008). However, the geological factors that controlled the gas hydrate accumulation in KG offshore basin are not known.

Worldwide analyses of the occurrence and distribution of gas hydrate deposits show that the fluid venting areas are the potential sites of gas hydrate accumulation (Mazurenko and Soloviev, 2003). The areas of fluid venting may be controlled by the tectonic settings of the region. For example, structures formed due to salt or shale tectonics govern the occurrence of gas hydrate in northwestern Gulf of Mexico slope and Niger Delta front (Hovland et al., 1997; Milkov and Sassen, 2001). The seismic character of fluid/gas movement like acoustic voids, acoustic chimneys and acoustic turbid layers can be mapped using high resolution seismic data (Hovland and Curzi, 1989; Kaluza and Doyle, 1996). The relationship between seabed morphology with shallow gas venting features are well known from Mid Norway, Nile deep-sea fan, Costa Rica and Gulf of Cádiz (Hovland, 1990; Loncke, et al., 2004; Peterson, et al., 2009; Somoza et al., 2003). Therefore, we made an attempt to analyze the seabed morphology, shallow subsurface structures and shallow deposits in KG offshore basin using high resolution sparker (HRS), sub-bottom profiler (SBP) and multibeam swath bathymetry data and establish a link between these shallow features with known areas of gas hydrate accumulation and cold seeps. The deep structure obtained from multi-channel seismic data can help in understanding the geological and tectonic control on the origin of seabed morphology and gas hydrate deposits.

2. Data and Methods

Table 1 depicts the coverage of high resolution sparker, SBP and bathymetry datasets acquired during different cruises. The high resolution single channel seismic data was acquired using GeoSpark 10 kJ system onboard Sagar Nidhi (SN21) in KG offshore basin for gas hydrate studies. The public domain software for Multibeam System 4.6.10 (Caress and Chayes, 1996) has been used to process and grid the swath bathymetry data. The GMT Software has been used to generate the color-coded contour maps on IBM P275 workstation with AIX 5.3 operating system. The HRS and SBP data were processed using seismic processing software “ProMAX” to generate enhanced seismic images. The SBP data has been used to infer the shallow deposits. Five echo facies are identified in the study area based on the classification of echo character (Damuth, 1975; Pratson and Laine, 1989). Long sediment cores (~30 m) collected onboard Marion Dufresne (MD161: May, 2007) in KG offshore basin are used to study the occurrence of vent related authigenic carbonates. The wet bulk density of the whole core was measured onboard using the GEOTEK Multisensor Core Logger (MSCL) system following standard calibration and measurement protocol (www.geotek.co.uk/ftp/manual.pdf). The density profiles are used to identify the zones of hard carbonate in the cores. Processed multichannel seismic (MCS) reflection data of 230 line kms acquired by Oil and Natural Gas Commission Ltd. (ONGC) have been used to study deep structures in KG offshore basin.

3. Stratigraphy and tectonic settings of KG basin

KG basin is a proven petroliferous basin of India which occupies an area of 28,000 sq. km onland and 145,000 sq. km offshore (Rao, 2001; Bastia, 2007). The thickness of the sediment in KG basin varies from 3-5 km in the onshore region and may exceed 8 km in the offshore region (Prabhakar and Zutshi, 1993). The study area (Fig. 1) lies in the continental slope region of KG basin, an integral part of the eastern continental margin of India (ECMI). ECMI evolved due to the breakup of eastern Gondwana landmass around 130 Ma when India separated from East Antarctica (Powell et al., 1988; Scotese et al., 1988; Ramana et al., 1994). As a consequence of rifting and drifting, three prominent offshore basins namely KG, Mahanadi and Cauvery were evolved along the ECMI. The KG basin is located in the middle of ECMI extending from Vishakhapatnam in the north to Ongole in the south and is filled with detrital sediments brought by Krishna and Godavari river system (Fig.1).

The general stratigraphy of the KG basin comprises of both syn-rift (Upper Jurassic to Early Cretaceous) and post-rift (Tertiary) petroleum systems (Rao, 1993). The sediment deposited during the syn-rift tectonic regime are lagoonal to fluvial and occasionally brackish water deposits (Ojha and Dubey, 2006). During late Jurassic, Gollapalli and Budavada sandstone got deposited in KG onshore basin under marginal marine settings (Sastri et al., 1973; Rao, 2001; Rao, 1993; Bastia, 2007). This unit is followed by Cretaceous Raghavpuram shale. During Paleocene epoch, onshore and offshore stratigraphy consists of Nimmakuru sandstone and Palakollu shale respectively. In KG onshore basin, sediment of Eocene epoch comprises of silty facies (Pasarlapudi Fm.), thick argillaceous limestones and dolomite formations (Bhimanapalli Fm.) followed by late arenaceous formation (Matsyapuri Fm.). Vadaparru shale was deposited in KG offshore basin during Eocene. A thin Oligocene layer (Narasapur claystone) overlies the Eocene unconformity. During Neogene period, increased sedimentation and subsidence rate coupled with lower sea level have deposited a thick sedimentary wedge. The onshore Rajamundry sandstone and offshore Ravva formation got deposited during Miocene. Andhra alluvium and Godavari clay comprises the onshore and offshore deposits of Holocene-Pleistocene epochs.

The tectonic activity along the ECMI resulted in the formation of several NE-SW trending horst and graben like structures and the structural fabric is controlled to a large extent by the direction governed by the Precambrian structural grain (Fig. 1). The subsidence model, based on well logs and seismic stratigraphy, suggests low sedimentation rates during Cretaceous (Subrahmanyam and Chand, 2006). High sedimentation and large subsidence rates were reported from Paleocene to Eocene due to the southeastward tilt of Indian plate and reversal of drainage pattern of major rivers (SubbaRao and Sukheshwala, 1981). Moderate subsidence was observed from Oligocene to Miocene due to marine transgression (Raju et al., 1999). The initial soft collision between the Indian and Eurasian plate, and subsequent uplift and erosion of Himalaya has dramatically increased the sedimentation rate during Neogene period.

4. Results

4.1 Bathymetric mounds and their association with gas hydrates/cold seeps

The shaded relief image of the bathymetric mosaic in KG offshore basin is shown in Fig. 2. The available drill/core locations from JOIDES Resolution and Marion Dufresne cruise are plotted on the bathymetric mosaic for comparison (Fig. 2a). The MCS, HRS and SBP lines that are illustrated in the

present study are superimposed on the interpreted bathymetry mosaic (Fig. 2b). The zoom out of the prominent bathymetric mounds (AA, BB and CC) are shown in the inset of Fig. 2b. The mounds are defined as the topographic high regions with smooth relief. Several oval-shaped bathymetric mounds of about 10 km long and 4 km wide (BB and CC in Fig. 2a) and rising to < 950 m from the surrounding 1050 m contour are observed. In the center, a circular mound (AA in Fig. 2a) having a diameter of 10-15 km and rising to < 650 m from the surrounding 900 m contour is observed. In the shallow (< 600 m) northeastern part of the study area, a delta front cut by numerous channels is observed. The bathymetry mosaic also shows a high relief sedimentary ridge with rugged topography. The sedimentary ridge is oriented in ENE-WSW direction and rises to < 1000 m from the surrounding 1300 m water depth. In the south-western part of the study area, a similar sedimentary ridge dominantly oriented in WNW-ESE direction is observed. This ridge rises to < 1100 m from the surrounding 1600 m water depth. All the observed ridges align in an arcuate shape probably restricting the free flow of sediment further offshore. The sediment ridges have distinct topography on either side. Landward, the sediment ridge shows smooth and low relief whereas in the offshore it is highly rugged with appreciable relief. It is interesting to note that all the bathymetric mounds which occur towards the landward side of the sedimentary ridges together form a slopebasin at the center of the study area. The bathymetry also shows evidences of two large-scale sedimentary deposits oriented in the coast-perpendicular direction. These deposits are characterized by undulatory, bulbous like topography and have a tongue like geomorphology. It appears that two tongue-like sediment lobes can be considered as a single system bifurcated by the sedimentary ridge at the center of the study area.

Drilling/coring results onboard JOIDES Resolution (Collett et al., 2008) confirm the presence of subsurface methane hydrate (> 10 % saturation as measured from pressure cores and/or estimated from resistivity logs) in NGHP-01-10/12/13/21 (J10 in Fig. 2a), NGHP-01-05 (J5), NGHP-01-14 (J14), and NGHP-01-15 (J15). It is interesting to note that these gas hydrate deposits occur close to the bathymetric mound (Fig. 2a). In contrast, cores NGHP-01-03 (J3) and NGHP-01-04 (J4) located in the slopebasin show either traces or no indications of hydrates.

The wet bulk densities of the sediment cores collected in KG offshore basin onboard Marion Dufresne (MD161) can be broadly classified into two categories based on the presence of hard authigenic carbonates. Density profiles (Figs. 3a-c) of Stns MD161/3, 8 and 15 located in the proximity of bathymetric mounds show a major and sharp increase in density at different depth zones and the

visual examination of sediment cores at these depths shows hard carbonates chunks. The visual examination of the core at Stn MD161/8 reveals authigenic carbonates of different morphology such as massive mudstone concretions, vacuolar mudstone concretions with gas flow channels, tubular and vase-shaped bioturbation casts with or without laminations, cemented breccias, chimneys and nodular types (Mazumdar et al., 2009). Furthermore, the presence of well preserved chemosynthetic clam, *callyptogena sp.* and depleted carbon isotopic values ($\delta^{13}\text{C}$ ranges from -41 to -52 ‰ VPDB) from these carbonates confirmed methane venting in KG offshore basin (Mazumdar et al., 2009). Wet bulk density profiles of sediment cores located in the intraslope basin (Stns MD161/7, 10 and 11 in Figs. 3d-f) are devoid of any sharp increase in density. The visual examination of these sediment cores reveals minor amounts of authigenic carbonates. No indication of gas hydrate is observed in the long sediment cores (~ 30 m) collected onboard Marion Dufresne.

4.2 Shallow subsurface expression of bathymetric mounds in high resolution seismic data

The high resolution sparker data having vertical (~2 m) and horizontal resolution (~85 m) and shallow depth of penetration (100-400 m) are used to infer the shallow subsurface structures of these mounds (Fig. 4). In the study area, a good correlation is observed between surficial expression as seen in bathymetry data and shallow structures as inferred from HRS and SBP data. In general, the mounds are characterized by two distinct sets of subbottom reflectors in the HRS data; one set shows parallel continuous reflector representing the folded overburden, while the other set is an acoustically transparent mass that is conformable to the seafloor and onlaps onto the parallel continuous reflector and shows prolonged bottom echo (Figs. 4a-c). The parallel continuous reflectors which represent finely layered sediment show the following characteristics: a) they are folded and the crest of the fold protrudes out of the seafloor to form the bathymetric mound, b) the folded overburden is extensively faulted and these faults may act as conduits for the movement of fluid/gas, c) the faulted overburden show chaotic reflections in a narrow zone of 50-100 m wide which can be interpreted as acoustic voids (Hovland and Curtzi, 1989). This acoustic voids represent overpressured sediment containing high concentration of dissolved gases or gases in bubble form leading to attenuation of seismic energy, d) some of the blocks have been uplifted by about 35-40 m (Figs. 4b and 4d). A block of ~ 50 m wide have been uplifted by about 25 m above the seafloor (Fig. 4c). In the study area, an uplift of 30-40 m is common on top of the mounds through fault system. It is interesting to note that the HRS data on top of the mound 'AA' (Fig. 4d) shows a massive fault-bounded gas upthrust structure which is a part of the major feature mapped on

the bathymetry (Fig. 2). The block comprises of layered and folded sediment and the bottom of the sediment is masked by an acoustically turbid layer around 1.26 s TWT. This turbid layer may be interpreted as gas charged sediment consisting of densely-spaced scatterers capable of absorbing the seismic energy (Hovland and Curtzi, 1989). Some more examples of fluid/gas related morphologies in the vicinity of the mounds are shown in Figure 5. Narrow regions of acoustically transparent zone which are classified as acoustic chimneys are observed. The mounds show the signatures of fluid/gas movements in the forms of acoustic voids, acoustic chimneys and acoustic turbid layer. Numerous growth-related faults are observed in the shallow sediment. Acoustic blanking is also observed beneath some mounds which may be related to the formation of gas hydrate (Lee and Dillon, 2001).

4.3 Shallow deposits in KG offshore basin

We have identified five different echo facies in KG offshore basin based on the classification suggested by Damuth (1975), Damuth and Hayes (1977) and Pratson and Laine (1989). The distribution of each echo facies is in agreement with the bathymetry mosaic. The echo characters observed along a regional coast-perpendicular HRS line (Fig. 6) can be subdivided into distinct zones such as delta front, mass transport deposit, mound, minibasin and sedimentary ridge. The HRS data across the delta front is characterized by distinct surface echo with several parallel, continuous subbottom reflections that are conformable to seafloor topography (Fig. 7a). The faults in the delta front region have facilitated the slumping and associated mass transport deposits towards the offshore region. The change in echo facies from distinct bottom echo with parallel subsurface layers to prolonged echo with overlapping hyperbolae is shown in Fig. 7a. This transition is clearly observed in the bathymetry data and can be mapped on the regional scale. The downward throw of sediment across the transition zone is more than 70 m.

Beyond 600 m water depth, the deposits are characterized by prolonged bottom echo with overlapping hyperbolae having small separation between the vertices (Fig. 7b). However in the northeastern part of the study area such deposits are characterized by prolonged bottom echo with acoustically transparent mass having few internal reflectors (Fig. 7d). In the bathymetry mosaic these sedimentary deposits show a tongue like geomorphology. The sedimentary ridges are characterized by discrete bottom echo with irregular hyperbolae having widely spaced vertices (Fig. 7c). The sediment piled up in this zone may extend up to 500 m above the surrounding seafloor. In the northeastern part of

the study area, folded and faulted strata are seen buried beneath the seafloor and can be identified in the HRS data (Fig. 7d). The parallel reflectors are faulted and show buried acoustic voids, and some of the blocks are uplifted. The overlying sediment is acoustically transparent mass with few internal reflections onlaps onto the buried mound. Moving seaward from the sedimentary ridges; we observed a change in echo facies from acoustically transparent masses to distinct bottom echo with several parallel to subparallel continuous reflections (Fig. 7e). This region appears to be gently dipping with no significant relief in the bathymetry mosaic.

4.4 Deep structures beneath the mounds as observed in MCS data

Processed and interpreted reflection seismic data crossing the prominent bathymetric mounds are shown in Figs. 8 and 9. The location of seismic line shown in Fig. 8 is same as that of HRS data (Fig. 6). Fig. 8 shows folded strata between CDPs 1100-1200 (corresponding to bathymetric mound) which exhibits a relief of 300-400 m. A similar pattern of folding of the subsurface layers is also observed between CDPs 200-500 and 1830-2000. Wavelength of the folded strata varies from 1.8 – 2.8 km and the depth of the folded strata is about 3 s. It is interesting to note that below the folded overburden a region of no coherent reflections bounded by sharp truncation of adjacent coherent reflectors is observed. This zone rises from 6.0 s deep upto 2-2.5 s in the overburden sediment. The observed folding of the subsurface layers is the result of upthrusting. The folded overburden is associated with major and minor fault systems between 1.0 and 2.0 s. The fault system between CDPs 1100-1400 is distributed radially with basinward dominance. Fig. 8 shows folded-faulted strata on the right between CDPs 1600-1700. High angle thrust fault ($\sim 57^\circ$) occurs close to the crest of slightly folded subsurface sediments. The hanging wall is thrust upward and seaward up to the seafloor indicating compression tectonics. The faulting has formed a minibasin which is filled with sediments; the reflectors within this basin are conformable to the seafloor and onlap onto the folded strata (Fig. 8 and Fig. 6). A similar fault can be inferred by the discontinuity of the underlying reflections below 4 s. However, the presence of multiples between 2-4 s does not allow the continuous identification of the fault. We believe that the faults in the upper and lower part of the section are part of a single fault extending from 5 s to the surface.

Some more examples of seismic lines crossing the bathymetric mound (AA and BB) are shown in Fig. 9. Seismic data shows folding and intense faulting of the subsurface layers beneath the

bathymetric mounds. Wavelength of the folded strata varies from 4 – 8 km and the depth of the folded strata is between 1-1.5 km. Below AA mound, the overburden is folded and around 3 to 4 s we observe a zone of no coherent reflections whose boundary is demarcated by abrupt truncation of coherent reflections. This zone is mushroom shaped with a narrow neck. The overburden seems to be faulted, two major faults above the mushroom shaped zone have uplifted the sediment block of approximate dimension of 4×1.2 km creating mound AA. Like-wise we observe zones of no coherent reflections below mound BB and another mound between CDPs 500-800 which appear to be uniform. It is interesting to note that the zones of no coherent reflection originates between 4.5-5.5 s.

The extensively faulted subsurface layer beneath the mounds provides a geologically conducive environment for the movement of fluid/gas. If the fluid/gas passes through the hydrate stability zone, it will form gas hydrate which will be manifested in the form of Bottom Simulation Reflectors (BSRs). BSRs represent a phase boundary between high-velocity hydrate bearing sediments and low-velocity gas charged sediments (Singh et al., 1993). The BSR mimics the seafloor topography and shows opposite polarity compared to that of the seafloor (Shipley et al., 1979). We have identified BSRs in the seismic profiles in the vicinity of the mounds as they show reverse polarity and cross cut the existing geological strata (see insets in Figs. 8 and 9). However, no BSRs are observed between CDPs 200-500 in Fig. 8 and 1600-1900 in Fig. 9 as the shallow bathymetry lies outside the hydrate stability zone.

5. Discussion

5.1 Origin of the bathymetric mound

The analysis of HRS, SBP and bathymetry data facilitated the identification and mapping of seabed mounds which show gas venting features (acoustic voids, acoustic chimneys, acoustic turbid layer and fault bounded gas upthrust structures) in continental slope regions of KG offshore basin. A map illustrating various structural features and shallow deposits is presented and the drilling/coring locations of JOIDES Resolution (NGHP cores labeled as J) and Marion Dufresne (MD 161 cores labeled as M) are highlighted (Fig. 10). The close association of the mounds with the seismic features indicative of fluid/gas movement strongly suggests that the seafloor mounds are related to fluid/gas movement. Hovland (1990) also observed that formation of seafloor morphological features in the continental margin off Mid Norway is related to gas seepage. Similarly, several bathymetric mounds of sizes ranging from 800-1200 m with evidences of fluid flow are reported from the continental slope off Costa

Rica (Peterson et al., 2009). A direct correlation between the mud mounds of size ranging from 1-2 km and 100 m relief and mud diapirism was established in Gulf of Cádiz (Fernández-Puga et al., 2007; Somoza et al., 2003). Geophysical studies of Nile Deep Sea Fan (NDSF) in Eastern Mediterranean show widespread regions of mounds and pockmarks associated with fluid flow features due to shale/salt induced gravity tectonics (Loncke et al., 2004).

In order to understand the origin of the mounds, we studied the deep structures beneath the mound using MCS data. The subsurface layers below the mounds are folded and zones of no coherent reflections are observed between 2 – 6 s. The zone of no coherent reflections seems to be originating between 4 and 5 s TWT below seafloor. Assuming an average velocity of 1900 m/s, the sediment thickness from the base of this zone is about 3.8 – 4.7 km and a sedimentation rate of 30-40 cm/kyr (ONGC Personal communication), we calculate that this zone is originating from the sedimentary layer of ~10-16 Ma (Middle-to-Late Miocene). The pressure profiles of wells drilled in KG basin show that Miocene sequence has abnormal formation pressure of more than 1.5 MWE (Mud Weight Equivalent) due to high sedimentation rate during Miocene (Rao, 1993; Rao and Mani, 1993). This Miocene depositional system in KG basin is reported to produce shale bulges in the deep offshore regions (Vijayalakshmi, 1988). The compaction trends obtained from seismic velocity also suggest that Mio-Pliocene sequences are overpressured in KG offshore basin (Basu, 1990). The study area is located on the continental slope region where overpressured shale sequences are known to cause shale diapirism due to gravity driven compression tectonics (Vijayalakshmi, 1988; Rao and Mani, 1993; Bastia, 2006; Gupta, 2006). Based on the available geological information, we suggest that the zones of no coherent reflections might be related to Miocene shale diapirism. Shale diapirism occurs due to downward movement of thick sediment mass over a deeply buried mobile shale strata (Bruce, 1973; Dailly, 1976; Evamy et al., 1978; Doust and Omatsola, 1990; Damuth, 1994; Morley and Guerin, 1996; Wu and Bally, 2000). Similar occurrence of mud diapirs have been reported along the continental margin of India (Vaz, 2001). The regional seismic lines in KG basin (cf. Fig. 8 in Bastia, 2006) show extension, translation and compression zones similar to that of Nigerian continental margin (Damuth, 1994) which represent a well studied region for shale tectonism. Large-scale Paleogene and Neogene growth faults, a characteristic of the extension zone, are also reported from KG basin in the continental shelf and upper slope regions (Rao and Mani, 1993; Bastia, 2007).

The illustrated seismic lines depict various forms and shapes of shale diapirs in KG offshore basin which are common in gravity-driven shale tectonics (Emery et al., 1975; Evamy et al., 1978; Damuth, 1994). The upward movement of diapir resulted in folding, faulting and upthrusting of the overburden strata thereby creating prominent bathymetric mounds. These mounds are associated with the fluid/gas movement as suggested by HRS and SBP data. In the northwestern part of the study area such surficial expressions are relatively subdued to deeper level due to the burial of mound by recent mass flow deposits.

Upward movement of diapirs results in the development of slope/marginal basins which usually are filled with sediments derived from upper continental slope or mass wasting of mounds formed due to diapirism or mass transport deposits. The location of seismic section depicting one such intraslope basin is shown in Ramana et. al. (2009). These deposits fill the intraslope basin and eventually spill over the diapiric mounds. In shale tectonics, deep offshore regions are characterized by toe-thrust faults and the sediments of slope regions are upthrust piercing through the seafloor (Damuth, 1994). We interpret the sedimentary ridges observed in the bathymetry mosaic to be the result of toe-thrust faulting. The landward facing surface of the ridge appears to be smooth because of the spilling over of the sediments from the intraslope basin. The detailed characterization of shale diapirs and toe-thrust fault in KG offshore basin requires closely spaced multi-channel seismic data or 3D seismic data and is beyond the scope of the paper.

5.2 Structural control on the accumulation of gas hydrate deposits and associated cold seeps

The seismic profiles show BSRs in the proximity of diapiric mounds and toe-thrust sedimentary ridges (see insets in Figs. 8 and 9). In this study, we identified mounds associated with fluid/gas movements probably related to the shale diapirism. The prevalence of shale diapirism indicates an unstable nature of KG basin and provides conducive geological environments for the movement of fluids/gas through fault system. Since the potential of hydrate accumulation increases if the region is structurally deformed, we believe that the shale diapirs and toe-thrust regions are favorable locales for gas hydrate formation. The localized fluid advection near shale diapiric mounds might have led to the observed gas hydrates accumulation in KG offshore basin. In Nigerian continental margin, similar shale tectonism has produced massive gas hydrate formation in the deep and ultradeep waters (Brooks et al., 2000).

We also observe that shale diapirs and toe-thrust zones are the regions of methane venting, precipitation of hard authigenic carbonates, and proliferation of chemosynthetic community. Sediment cores collected in mud diapiric region MD161/8 and 15 (M8 and M15 in Fig. 10) and toe-thrust zone MD161/3 (M3) show the presence of authigenic carbonates as indicated by an abrupt increase in wet bulk density profiles (Fig. 3a-c). The visual examination of sediment core at Stn MD161/8 depicted authigenic carbonates of different morphology and geochemical analysis of these carbonates show depleted carbon isotopic values ($\delta^{13}\text{C}$ ranges from -41 to -52 ‰ VPDB) (Mazumdar et al., 2009). The presence of chemosynthetic community *callyptogena sp.* confirms that paleo-cold seeps in KG offshore basin (Mazumdar et al., 2009). Similar cold seep locations and high methane flux are reported from Gulf of Mexico where the salt diapir creates numerous faults which act as pathways for the fluid/gas migration resulting in several hydrate mounds associated with chemosynthetic community (Sassen et al., 1998). We believe that the folded/faulted and upthrustsed overburden sediment due to shale diapirism facilitate the formation of cold seeps in KG offshore basin. The cold seeps and methane venting may be considered as reliable surficial proxies of methane hydrate deposits in the subsurface (Sassen et al., 1998). In contrast, cores collected in the intraslope basin MD161/7, 10, and 11 (Fig. 10) show little or no indication of hard authigenic carbonates in wet bulk density profiles (Figs. 3d-f) suggesting that such basins might be devoid of surficial proxies for methane venting.

We propose a geological model for the formation and distribution of gas hydrate in the KG offshore basin (Fig. 11). Initially, low permeable (mostly clay), stratified sedimentary package with high total organic content (TOC) got deposited which has the potential to produce methane gas upon burial (Fig. 11a). The observed TOC (1-1.5 %) of the sediment in KG basin (NIO, 2005) is adequate to produce significant quantity of biogenic gas. The measurement of gas composition from the pressure cores collected in KG offshore suggests that the methane gas trapped in the hydrate layer is of biogenic origin (Collett et al., 2008). The upward movement of diapir due to shale tectonism causes the folding/faulting and upthrust of overburden sediment creating numerous mounds. The movement of fluid/gas through this fault system has led to localized high gas saturation close to the faults (Fig. 11b). Intraslope basins are formed synchronously and begin to fill with sediment derived from the continental margin. Due to movement of fluid/gas near the mud mounds, hydrates are preferentially deposited around these mounds and focused fluid flow in the fault zones might have led to the expulsion of methane and sulfidic rich fluids to form cold seeps (Fig. 11c). Based on the present study, we believe

that the gas hydrate accumulations in NGHP-01-10 and NGHP-01-5, and cold seep formations in MD161/8 and MD161/15 locations are representative of this scenario. Eventually, the mud mounds will get buried under the sediment after the intraslope basins are filled (Fig. 11d). We believe that the gas hydrate system in NGHP-01-15 site represents a subdued diapiric mound. The proposed model is conceptually similar to the one proposed by Hovland (1990) for the continental slope off Mid Norway. However, the model differs in three aspects i) the location of the seafloor mounds is controlled by deeply buried Miocene shale diapirs; ii) intense subsurface faulting due to upward thrust of diapirs are clearly observed in the seismic data and iii) the presence of gas hydrate in the sediment increases the stability of the sediment and prevent expulsion of gases into the water column. In the study area, we have not observed any seismic signatures akin to mud volcanoes, which is common in shale diapirism (Fernández-Puga et al., 2007; Somoza et al., 2003) probably because of the presence of gas hydrate in the slope regions.

5.3 Shallow depositional environment in KG offshore basin

In KG offshore basin, we observe that the shallow deposits are also linked with shale tectonism. The delta-front lobe is characterized by parallel continuous reflectors which is a characteristic feature of detrital/hemipelagic deposits. The delta-front lobe is seen cut by numerous channels which might have deposited the sediments in the intraslope basin. The slope basins are filled with acoustically transparent masses having a few internal reflectors. Such acoustically transparent masses have been interpreted elsewhere as mass transport deposits (Embley, 1976; Damuth, 1980). Following the classification/concept of Damuth (1994), the KG basin can be categorized into three zones: a) regions affected by extensional faults as extensional zones, b) regions affected by shale/mud diapirs as translation zones, and c) zones affected by compression tectonics as compression zone. A study pertaining to the extension zone is outside the region of interest in this paper. In the translation zone, several mud mounds formed due to shale diapirism are identified in the MCS, HRS, and bathymetry data. In the compression zones, folding, faulting and upward movement of sediment masses have created prominent toe-thrust sedimentary ridges. The observed sedimentary ridge exhibits indistinct bottom echo with no subsurface reflections. At the base of the compression zone towards offshore, the bathymetry texture changes from highly rugged, faulted to planar and quintessence. Several parallel to subparallel continuous subbottom reflections with distinct bottom echo are observed in this zone thereby indicating a low energy depositional environment.

6. Conclusions

We identified and mapped bathymetric mounds which are associated with fluid/gas migration features such as acoustic chimneys, acoustic voids and acoustic turbid layer in KG offshore basin based on the analysis of HRS, SBP and bathymetry data. The HRS and bathymetry data resolved the finer details and regional extension of these features while MCS data helped in establishing the broader framework for the origin of mounds. We propose the mounds are formed due to an upward movement of Miocene shale diapirs based on the analysis of MCS profiles and the available geological information. The upward movement of diapirs has produced numerous faults/fractures in the overburden which facilitate the accumulation of gas hydrate and formation of cold seeps. Drilling/coring through diapiric mounds has confirmed the presence of subsurface gas hydrate and cold seeps. In contrast, no good gas hydrates proxies could be discerned in the intraslope basins though they are filled with thick sediment and lie within the gas hydrate stability zone probably due to the lack of tectonically related migration pathways.

Acknowledgements We thank the Directors of National Institute of Oceanography (NIO), National Institute of Ocean Technology (NIOT), National Center of Antarctica and Ocean Research (NCAOR) and Secretary, Ministry of Earth Sciences (MOES) for supporting this study. Head Oceanography Department, IPEV provided technical support and facilities onboard Marion Dufresne. We thank oil industry for providing valuable multi-channel seismic data. We thank Dr. Martin Hovland, Dr. Cornel Olariu and two anonymous reviewers for providing constructive comments/suggestions which have improved the quality of the manuscript. This is NIO contribution no. xxx.

References:

- Bastia, R., 2006. An overview of Indian sedimentary basins with special focus on emerging east coast deepwater frontiers. *The Leading Edge* 25, 818–829.
- Bastia, R., 2007. *Geologic settings and petroleum systems of India's east coast offshore basins: Concepts and Applications*. Technology Publication, Dehradun, India.
- Basu, S., 1990. Clay mineralogy and pressure analysis from seismic information in Krishna-Godavari basin, India. *Geophysics* 55, 1447-1454.
- Brooks, J.M., Bryant, W.R., Bernard, B.B., Cameron, N.R., 2000. The nature of gas hydrates on the Nigerian continental slope. *Annals of the New York Academy of Sciences* 912, 76–93.
- Bruce, C.H., 1973. Pressured shale and related sediment deformation; mechanism for development of regional contemporaneous faults. *AAPG Bulletin* 57, 878–886.
- Caress, D.W., Chayes, D.N., 1996. Improved processing of hydrosweep DS multibeam data on the R/V Maurice Ewing. *Marine Geophysical Researches* 18, 631–650.
- Collett, T.S., et al., 2008. Results of the Indian National Gas Hydrate Program Expedition 01 initial reports, Dir. Gen. of Hydrocarbons, Min. of Pet. and Nat. Gas, New Delhi.
- Dailly, G.C., 1976. A possible mechanism relating progradation, growth faulting, clay diapirism and overthrusting in a regressive sequence of sediments. *Bulletin of Canadian Petroleum Geology* 24, 92–116.
- Damuth, J.E., 1975. Echo character of the western equatorial Atlantic floor and its relationship to the dispersal and distribution of terrigenous sediments. *Marine Geology* 18, 17–45.
- Damuth, J.E., 1980. Use of high-frequency (3.5-12 kHz) echograms in the study of near-bottom sedimentation processes in the deep-sea: a review. *Marine Geology* 38, 51–75.
- Damuth, J.E., 1994. Neogene gravity tectonics and depositional processes on the deep Niger Delta continental margin. *Marine and Petroleum Geology* 11, 320–346.
- Damuth, J.E., Hayes, D.E., 1977. Echo character of the East Brazilian continental margin and its relationship to sedimentary processes. *Marine Geology* 24, 73–95.
- Doust, H., Omatsola, E., 1990. Niger Delta In: Edwards, J.D., Santogrossi, P.A. (Eds.), *Divergent / passive margin basins*. American Association of Petroleum Geology Memoirs, vol. 48, pp. 201–238.
- Embley, R.W., 1976. New evidence for occurrence of debris flow deposits in the deep sea. *Geology* 4, 371–374.
- Emery, K.O., Uchupi, E., Phillips, J., Bowin, C.O., Mascle, J., 1975. Continental margin off western Africa; Angola to Sierra Leone. *AAPG Bulletin* 59, 2209–2265.

- Evamy, B.D., Haremboure, J., Kamerling, P., Knaap, W.A., Molloy, F.A., Rowlands, P.H., 1978. Hydrocarbon habitat of Tertiary Niger Delta. AAPG Bulletin 62, 1–39.
- Fernández-Puga, M., Vázquez, J., Somoza, L., Diaz del Rio, V., Medialdea, T., Mata, M., León, R., 2007. Gas-related morphologies and diapirism in the Gulf of Cádiz. *Geo-Marine Letters* 27(2), 213–221.
- Gupta, S.K., 2006. Basin architecture and petroleum system of Krishna Godavari Basin, east coast of India. *The Leading Edge* 25, 830.
- Hovland, M., 1990. Suspected gas-associated clay diapirism on the seabed off Mid Norway. *Marine and petroleum geology* 7, 267-276.
- Hovland, M., Curzi, P., 1989. Gas seepage and assumed mud diapirism in the Italian central Adriatic Sea. *Marine and petroleum geology* 6, 161-169.
- Hovland, M., Gallagher, J.W., Clennell, M.B., Lekvam, K., 1997. Gas hydrate and free gas volumes in marine sediments: Example from the Niger Delta front. *Marine and Petroleum Geology* 14, 245–255.
- Kaluza, M.J., Doyle, E.H., 1996. Detecting fluid migration in shallow sediments: Continental slope environment, Gulf of Mexico. In AAPG (Ed.), *Hydrocarbon migration and its near-surface expression*, Tulsa, 15–26.
- Lee, M.W., Dillon, W.P., 2001. Amplitude blanking related to pore-filling of gas hydrate in sediments. *Marine Geophysical Researches* 22, 101-109.
- Loncke, L., Mascle, J., Parties, F., 2004. Mud volcanoes, gas chimneys, pockmarks and mounds in the Nile deep-sea fan (Eastern Mediterranean): geophysical evidences. *Marine and Petroleum Geology* 21(6), 669--689.
- Mazumdar, A., Dewangan, P., Joao, H.M., Peketi, A., Khosla, V.R., Kocherla, M., Badesab, F.K., Joshi, R.K., Roxanne, P., Ramamurty, P.B., Karisiddaiah, S.M., Patil, D.J., Dayal, A.M., Ramprasad, T., Hawkesworth, C.J., Avanzinelli, R., 2009. Evidence of paleo-cold seep activity from the Bay of Bengal, offshore India. *Geochemistry Geophysics Geosystems* 10(6), 15 pp, doi:10.1029/2008GC002337.
- Mazurenko, L.L., Soloviev, V.A., 2003. Worldwide distribution of deep-water fluid venting and potential occurrences of gas hydrate accumulations. *Geo-Marine Letters* 23, 162–176.
- Milkov, A.V., Sassen, R., 2001. Estimate of gas hydrate resource, northwestern Gulf of Mexico continental slope. *Marine Geology* 179, 71–83.
- Morley, C.K., Guerin, G., 1996. Comparison of gravity-driven deformation styles and behavior associated with mobile shales and salt. *Tectonics* 15, 1154–1170.
- NIO, 2005. Geo-scientific investigations of shallow sediment in KG offshore, east coast. NIO/TR-13/2005. 103 pp.
- Ojha, P.S., Dubey, M., 2006. Gaint hydrocarbon fields of offshore Krishna-Godavari Basin. Petroview 1, published by Directorate General of Hydrocarbons, New Delhi , 26–30.

- Petersen, C., Klauke, I., Weinrebe, W., Ranero, C., 2009. Fluid seepage and mound formation offshore Costa Rica revealed by deep-towed sidescan sonar and sub-bottom profiler data. *Marine Geology* 266(1-4), 172-181.
- Powell, C.M., Roots, S.R., Veevers, J.J., 1988. Pre-breakup continental extension in east Gondwanaland and the early opening of the eastern Indian Ocean. *Tectonophysics* 155, 261–283.
- Prabhakar, K.N., Zutshi, P.L., 1993. Evolution of southern part of Indian east coast basins. *J. Geological Society of India* 41, 215–230.
- Pratson, L.F., Laine, E.P., 1989. The relative importance of gravity-induced versus current-controlled sedimentation during the Quaternary along the Mideast U. S. outer continental margin revealed by 3.5 kHz echo character. *Marine Geology* 89, 87–126.
- Raju, D.S.N., Bhandari, A., Ramesh, P., 1999. Relative sea level fluctuations during Cretaceous and Cenozoic in India. *ONGC Bulletin* 36, published by Oil and Natural Gas Corporation Limited, Dehradun, 185–202.
- Ramana, M.V., Nair, R.R., Sarma, K.V.L.N.S., Ramprasad, T., Krishna, K.S., Subrahmanyam, V., D'Cruz, M., Subrahmanyam, C., Paul, J., Subrahmanyam, A.S., Sekhar, D.V.C., 1994. Mesozoic anomalies in the Bay of Bengal. *Earth and Planetary Science Letters* 121, 469–475.
- Ramana, M.V., Ramprasad, T., Kamesh Raju, K.A., Desa, M., 2007. Occurrence of gas hydrates along the continental margins of India, particularly the Krishna-Godavari offshore basin. *International Journal of Environmental Studies* 64, 675–693.
- Ramana, M.V., Ramprasad, T., Paropkari, A.L., Borole, D.V., Ramalingeswara Rao, B., Karisiddaiah, S.M., Desa, M., Kocherla, M., Joao, H.M., Lokabharati, P., Gonsalves, Maria-Judith, Pattan, J.N., Khadge, N.H., Prakash Babu, C., Sathe, A.V., Kumar, P., Sethi, A. K., 2009. Multidisciplinary investigations exploring indicators of gas hydrate occurrence in the Krishna–Godavari Basin offshore, east coast of India. *Geo-Marine Letters* 29(1), 25-38
- Rao, G.N., 1993. Geology and hydrocarbon prospects of East Coast sedimentary basin of India with special reference to Krishna-Godavari Basin. *Journal of Geological Society of India* 41, 444–454.
- Rao, G.N., 2001. Sedimentation, stratigraphy, and petroleum potential of Krishna-Godavari Basin, East Coast of India. *AAPG Bulletin* 85, 1623–1643.
- Rao, G.N., Mani, K.S., 1993. A study on generation of abnormal pressures in Krishna-Godavari basin. *Indian Journal of Petroleum Geology* 2, 20–30.
- Somoza, L., Diaz-del-Rio, V., León, R., Ivanov, M., Fernández-Puga, M., Gardner, J., Hernández-Molina, F., Pinheiro, L., Rodero, J., Lobato, A., Maestro, A., Vazquez, J. T., Medialdea, T., Fernández-Salas, L.M., 2003. Seabed morphology and hydrocarbon seepage in the Gulf of Cádiz mud volcano area: Acoustic imagery, multibeam and ultra-high resolution seismic data. *Marine geology* 195(1-4), 153--176.

- Sassen, R., MacDonald, I.R., Guinasso, N.L., Joye, S., Requejo, A.G., Sweet, S.T., Alcala Herrera, J.A., DeFreitas, D.A., Schink, D.R., 1998. Bacterial methane oxidation in sea-floor gas hydrate; significance to life in extreme environments. *Geology* 26, 851–854.
- Sastri, V.V., Sinha, R.N., Singh, G., Murti, K.V.S., 1973. Stratigraphy and tectonics of sedimentary basins on East Coast of Peninsular India. *AAPG Bulletin* 57, 655–678.
- Scotese, C.R., Gahagan, L.M., Larson, R.L., 1988. Plate tectonic reconstructions of the Cretaceous and Cenozoic ocean basins. *Tectonophysics* 155, 27–48.
- Singh, I.B., Swamy, A.S.R., 2006. Delta sedimentation: East coast of India. Technology Publication, Dehradun, India.
- Singh, S.C., Minshull, T.A., Spence, G.D., 1993. Velocity structure of a gas hydrate reflector. *Science* 260, 204–207.
- Shipley, T., Houston, M., Buffler, R., Shaub, F., McMillen, K., Ladd, J., Worzel, J., 1979. Seismic evidence for widespread possible gas hydrate horizons on continental slopes and rises. *AAPG Bulletin* 63(12), 2204--2213.
- Sloan, E.D., 1990. Clathrate Hydrates of Natural Gases. Marcel Dekker, Inc., New York, 641 p.
- SubbaRao, K.V., Sukheshwala, R.N., 1981. Deccan volcanism and related basalt provinces in other parts of the world. *Geological Society of India Memoirs* 3, 474 pp.
- Subrahmanyam, C., Chand, S., 2006. Evolution of the passive continental margins of India—a geophysical appraisal. *Gondwana Researches* 10, 167–178.
- Vaz, G.G., 2001. Mud diapirs around Indian continental margin—Indicator of potential gas hydrate zone. *Current Science* 81, 245–246.
- Vijayalakshmi, K.G., 1988. Miocene depositional systems in thrust areas in Krishana-Godavari basin. *Bulletin of Oil and Natural Gas Corporation* 25(2), 1-10.
- Wu, S., Bally, A.W., 2000. Slope tectonics-comparisons and contrasts of structural styles of salt and shale tectonics of the northern Gulf of Mexico with shale tectonics of Offshore Nigeria in Gulf of Guinea. *Geophysical Monograph* 115, 151–172.

Table Caption

Table 1. Coverage of high resolution seismic, SBP and bathymetry datasets acquired during different oceanographic cruises. Swath bathymetry data was obtained during the Sagar Kanya (SK-176) and Marion Dufresne (MD161) cruises. SBP data was acquired during Marion Dufresne (MD161) and Sagar Nidhi (SN21) cruises. High resolution seismic data with 10 kJ sparker source was collected onboard Sagar Nidhi (SN21).

Figures Caption

Fig. 1. Location map of the study area in the KG offshore basin. A) Map of the regional tectonics setting showing the horst and graben structures (Rao, 2001; Bastia, 2006) onshore KG basin, Bay of Bengal. B) Coverage of multibeam swath bathymetry, multi-channel seismic, and high resolution seismic data in the study area. Thick solid lines show the track of available multi-channel seismic lines superimposed on the multibeam bathymetry data; blue lines show the track lines of high resolution sparker data acquired onboard Sagar Nidhi (SN21). The contour interval is 100 m

Fig. 2. Swath bathymetry mosaic acquired in the slope and rise regions of KG offshore basin (modified after Ramana et al., 2009). A) Shaded relief image of bathymetry mosaic along with the available drilling/coring locations and B) Interpreted bathymetry map showing the locations of illustrated MCS lines with CDP annotation (Figs. 8 and 9). The dashed dot line indicates the seismic line illustrated in Ramana et al. (2009). Blue lines represent the location of illustrated high resolution seismic data. The dashed black line indicates the large scale mass transport deposits having a tongue like geomorphology. Contour interval is 25 m.

Fig. 3. Wet density profiles of sediment cores collected onboard Marion Dufresne. The sharp increase in wet bulk density of the cores (MD161/3, 8 and 15) illustrates the zone of hard carbonate deposition. The locations of the Marion Dufresne cores are shown in Fig. 2. Detailed geological and geochemical analysis of carbonates in MD161/8 indicate the presence of paleo-cold seep in KG basin (Mazumdar et al., 2009).

Fig. 4. Subsurface manifestation of mounds as observed in the high resolution seismic data. The locations of the seismic lines are shown in Fig. 2b. The seismic data shown in plots A, B and D represent HRS data whereas plot B shows SBP data on top of the bathymetric mounds. The finely layered sediments are annotated as FLS and mass transport deposits as MTD. The bold arrow shows onlapping of MTD onto FLS. Several gas-escape related features such as acoustic voids and acoustic turbid layer are observed in the seismic data. Numerous fault-bounded, gas-upthrust structures ranging from 50 m – 8 km width and a relief of ~30-40 m are observed in the proximity of bathymetric mounds.

Fig. 5. Some more examples of HRS data on top of the mounds showing fluid/gas migration features such as acoustic voids, acoustic chimneys and acoustic turbid layer. Acoustic blanking due to the presence of gas hydrates is also observed close to mounds. The locations of the seismic lines are shown in Fig. 2b.

Fig. 6. A regional coast-perpendicular HRS profile highlighting various echo facies corresponding to delta front, mass transport deposits, mounds, minibasin and sedimentary ridges.

Fig. 7. Details of different depositional environments as deduced from echo facies analysis. The locations of the seismic lines are marked in Fig. 2b. A) Finely layered sediment (FLS) with faults showing submarine slope failure in KG offshore basin; B) Example of mass transport deposits in the slope basin regions; C) Imprints of toe-thrust sedimentary ridges in the SBP data; D) Subdued surficial expression of folded-faulted sediment in the north-western part of the study area; E) Finely layered sediment onlapping onto a basal reflector suggesting low depositional environment.

Fig. 8. Deep structure beneath the bathymetric mounds as observed in the multi-channel seismic lines collected in the continental slope regions of KG basin. A) Processed MCS data and B) interpreted seismic section. Green line represents the seafloor, yellow lines represent the predicted seafloor multiples and light blue lines are the interpreted BSR. Major seismic reflectors are shown using red lines. Zones of no coherent reflection originating at around 6 s and rising upto 2.2-2.4 s are observed between CDPs 200-500 and 1100-1200. High angle reverse fault is observed between CDPs 1600-1700 and the corresponding bathymetry appears to be undulated corresponding to sedimentary ridge. The insets shows the zoom out of the portion of the seismic section where BSRs are observed.

Fig.9. Same as Fig. 2 showing some more deep structures beneath the mounds in KG offshore basin. The folded overburden sediment protrudes out of seafloor forming prominent bathymetric mound. The zones of no coherent reflection seem to be originating around 5.5 s and rises upto 3-4 s. This zone has a mushroom shaped head and a narrow neck between CDPs 1600-1900 with two major fault systems that have uplifted the sediment block. Major and minor fault system develops radially in the folded overburden. The insets shows the zoom out of the portion of the seismic section where BSRs are observed.

Fig. 10. Shallow structures and depositional environment map based on the analysis of HRS, SBP and bathymetry data. Stars represent the location of the cores collected onboard JOIDES Resolution (labeled as J) and blue circles indicate the location of the cores collected onboard Marion dufresne (labeled as M). The red line indicates the transition from finely layered sediment to acoustic transparent masses and blue lines indicates the transition from high relief, rugged zones to planar bathymetry.

Fig. 11. A plausible geological model for the formation and distribution of gas hydrates in KG offshore basin. A) Burial of high TOC (1-1.5 %) sediment and microbial formation of methane gas at deeper sediment; B) Upward movement of shale diapirs leading to the folding and faulting of the overburden sediment and mobilization of fluid/gas; C) Formation of cold seeps and gas hydrate in the diapiric mound; and D) Burial of the diapiric mound as the sedimentation continues.

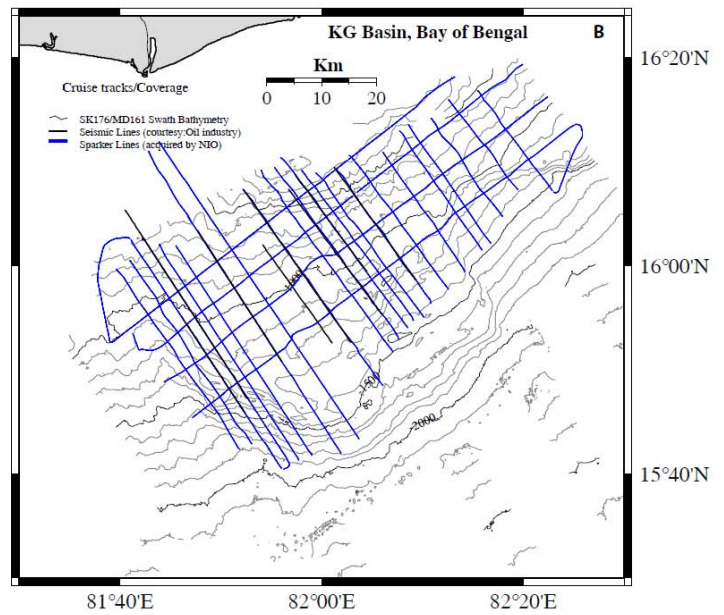
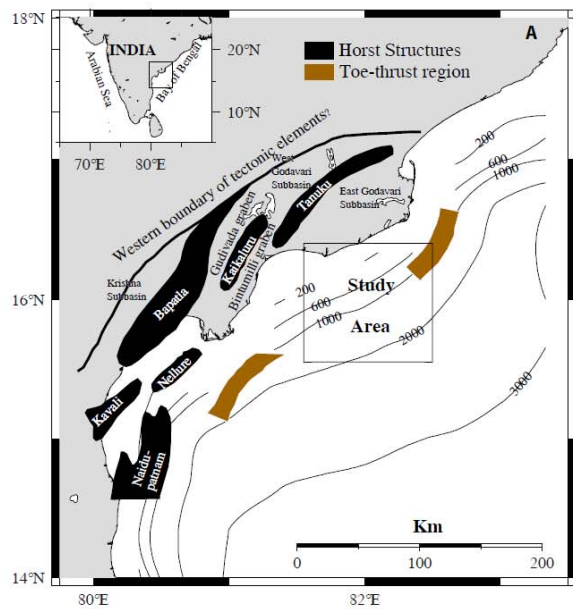


Figure 1

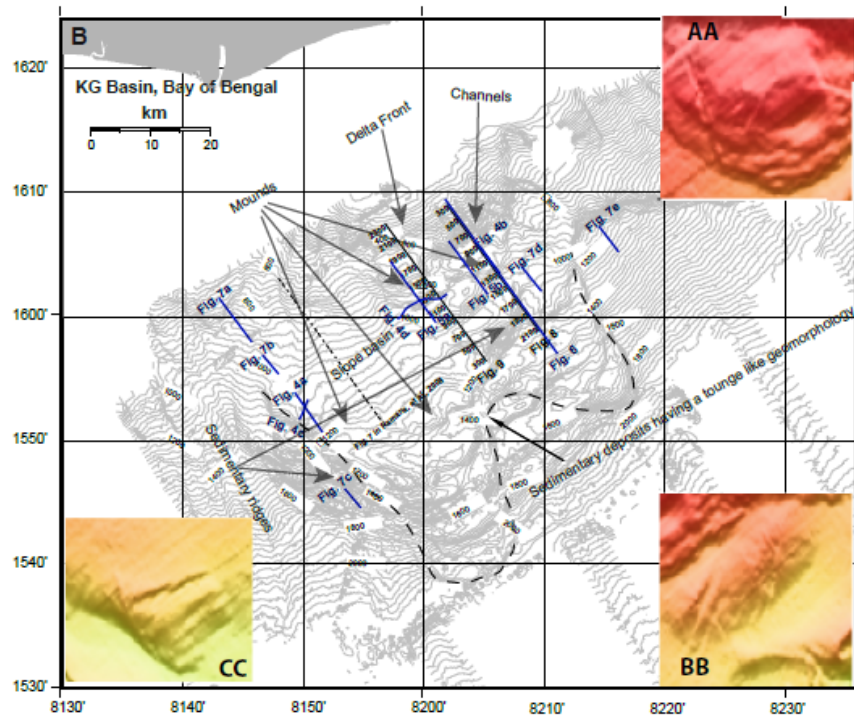
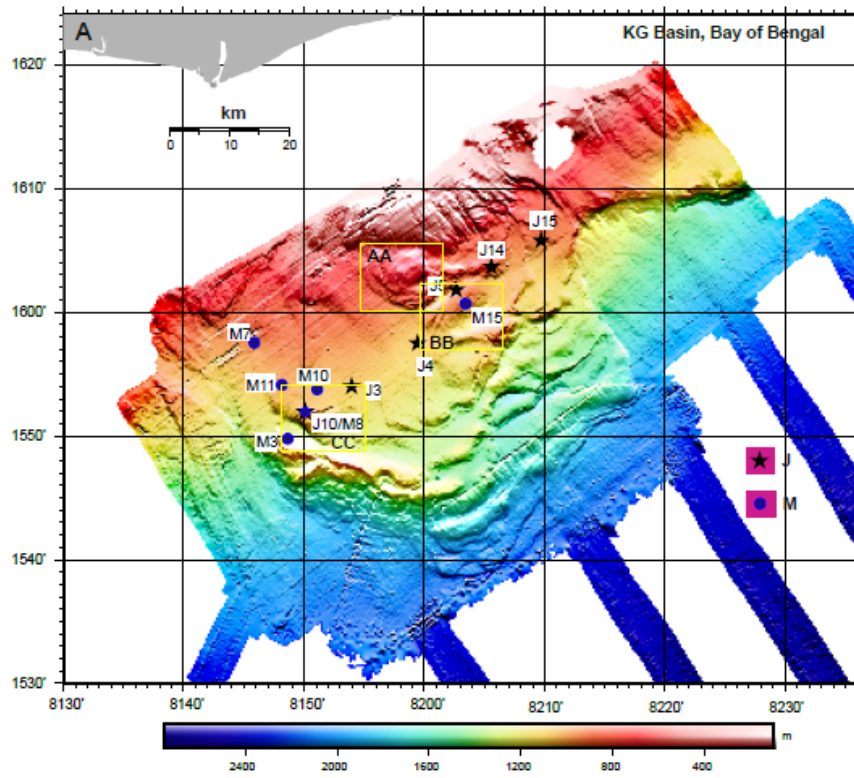


Figure 2

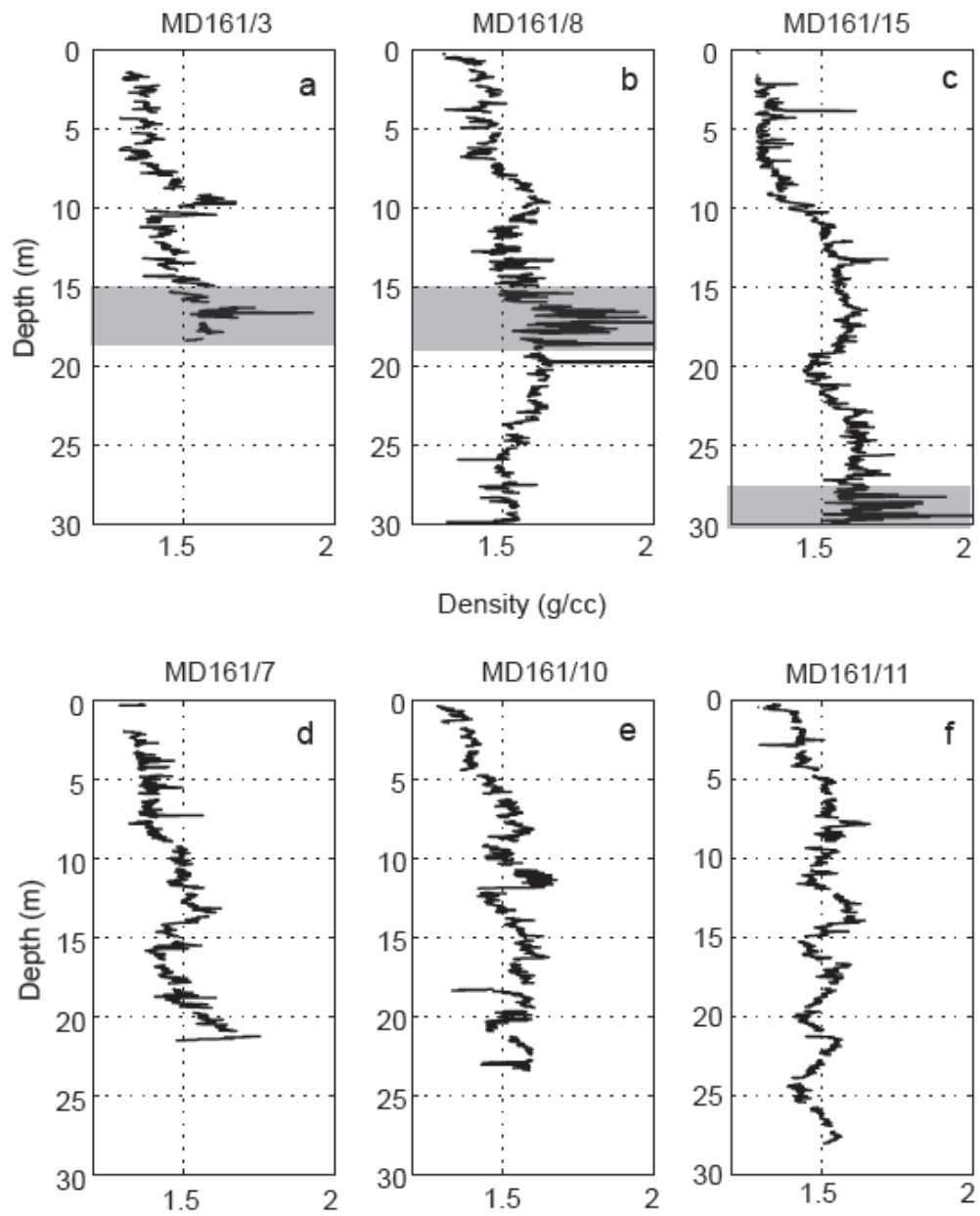


Figure 3

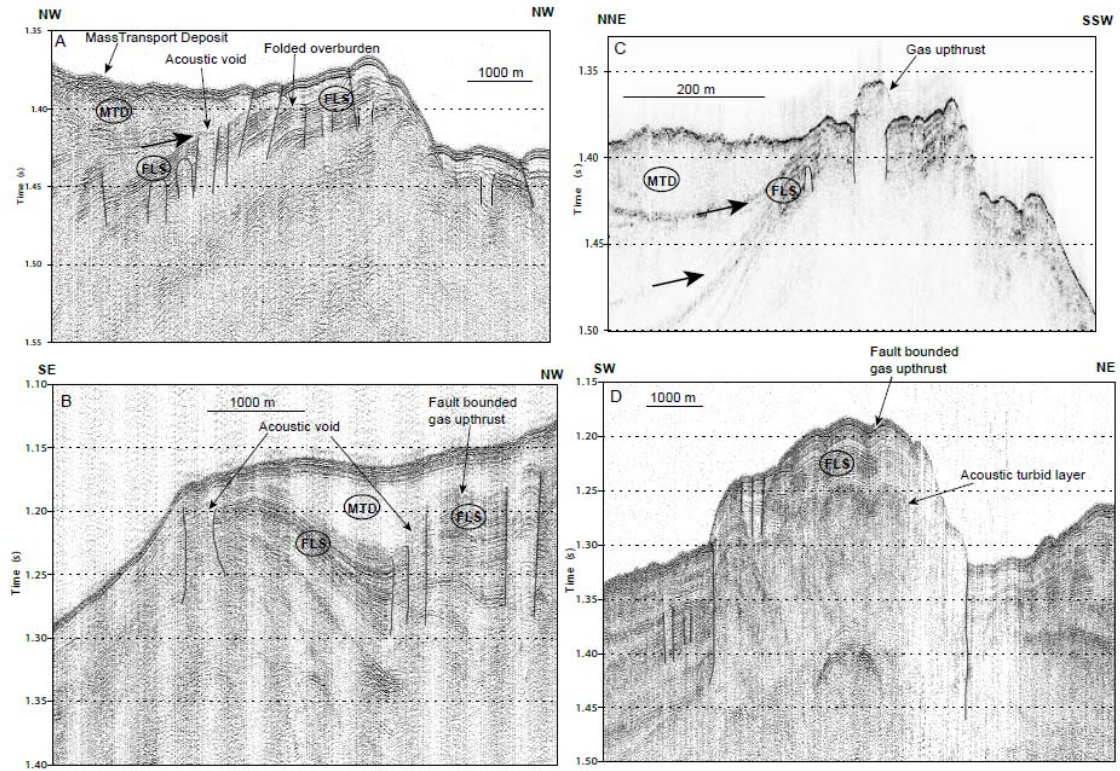


Figure 4

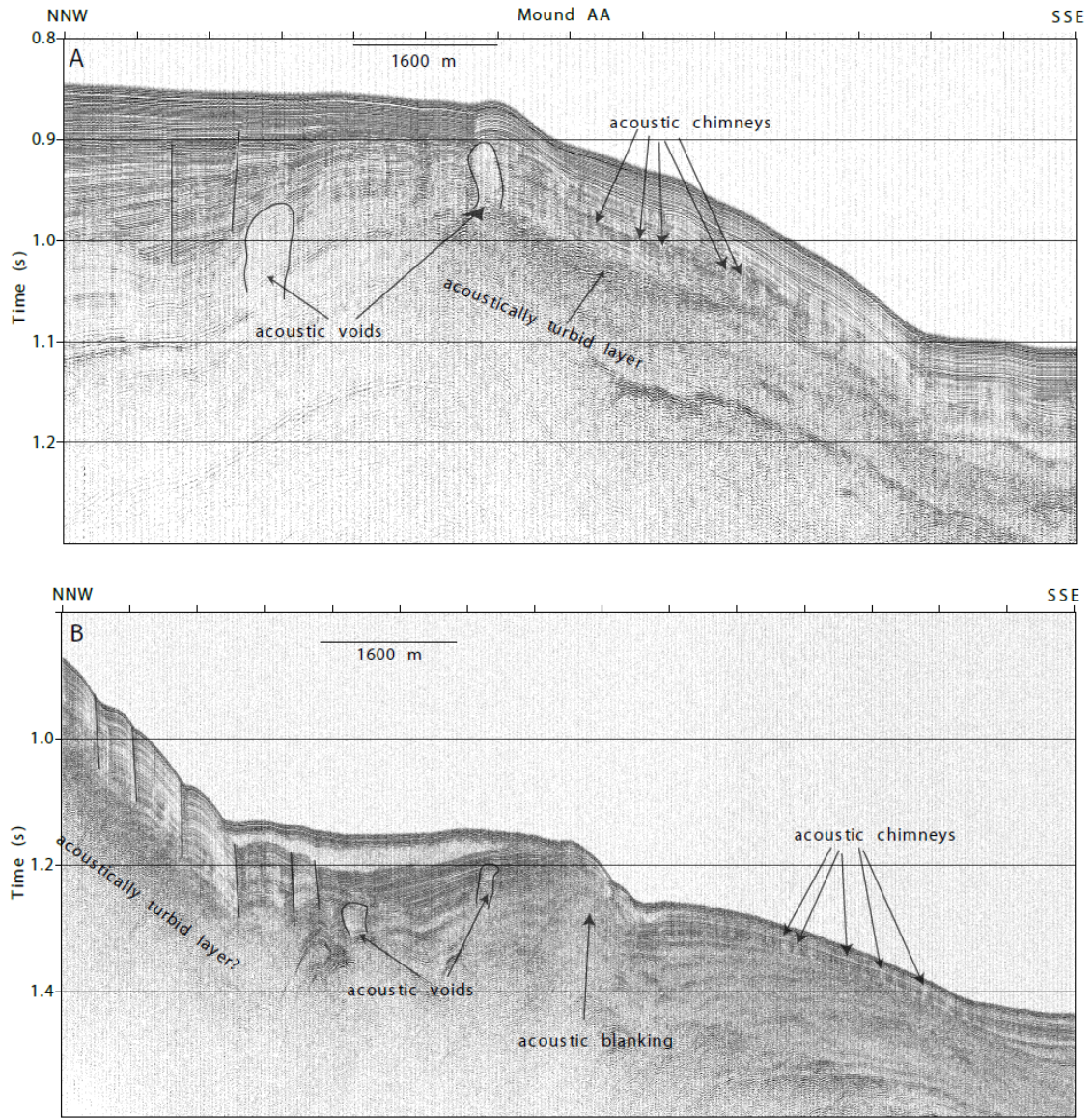


Figure 5

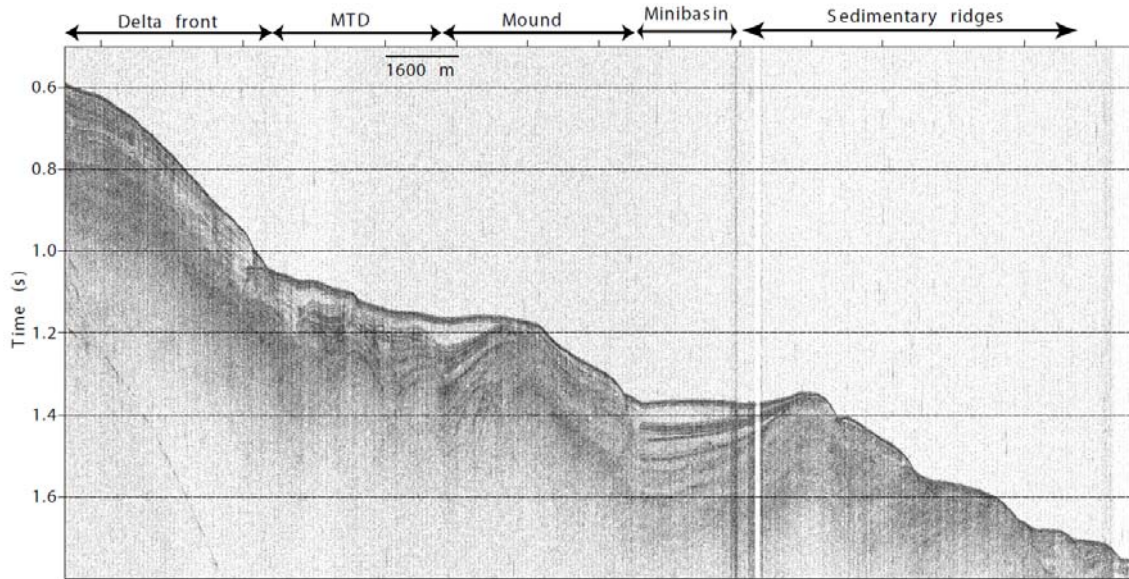


Figure 6

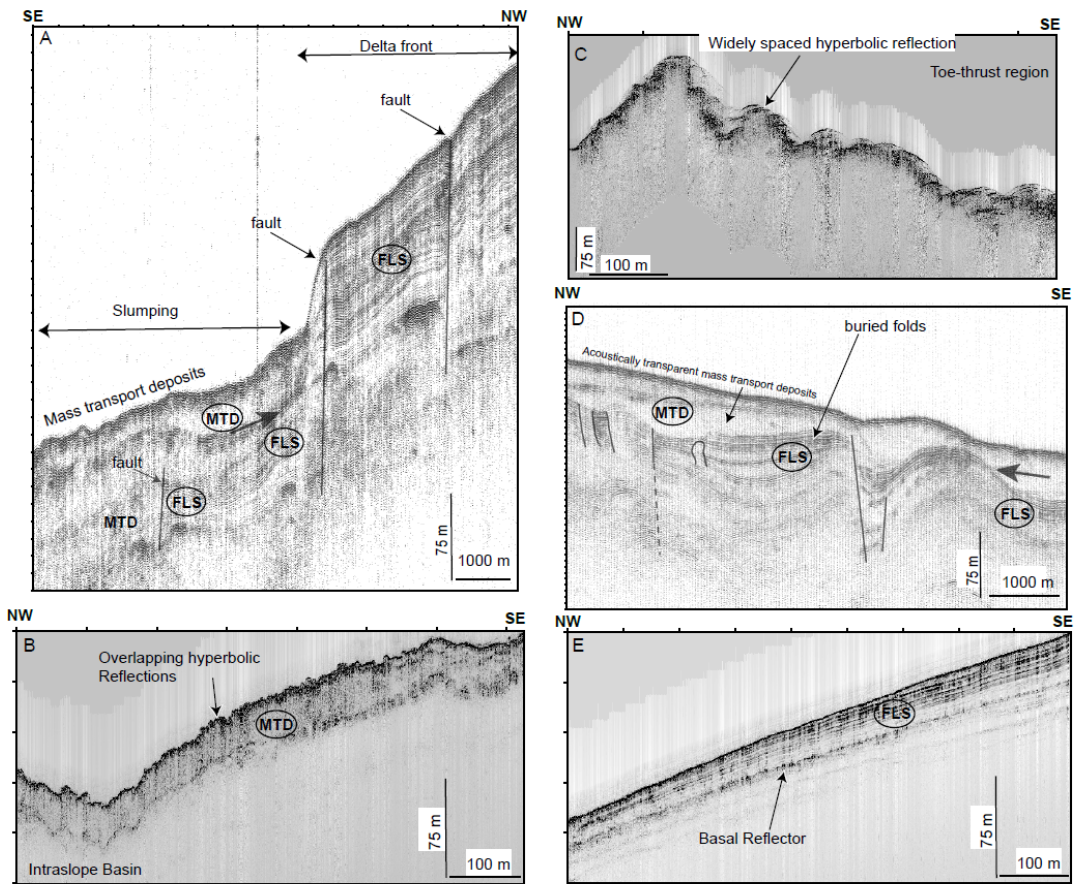


Figure 7

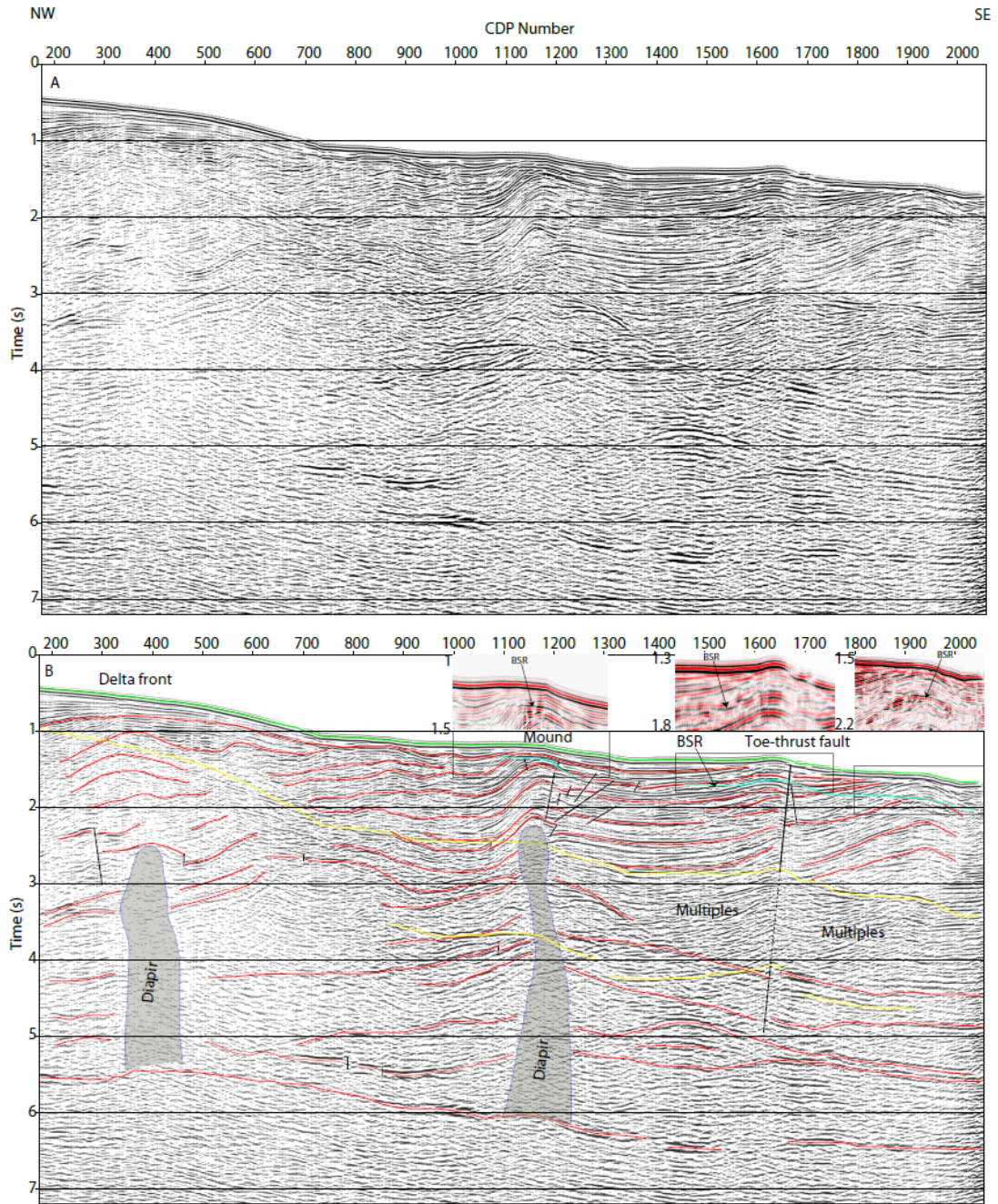


Figure 8

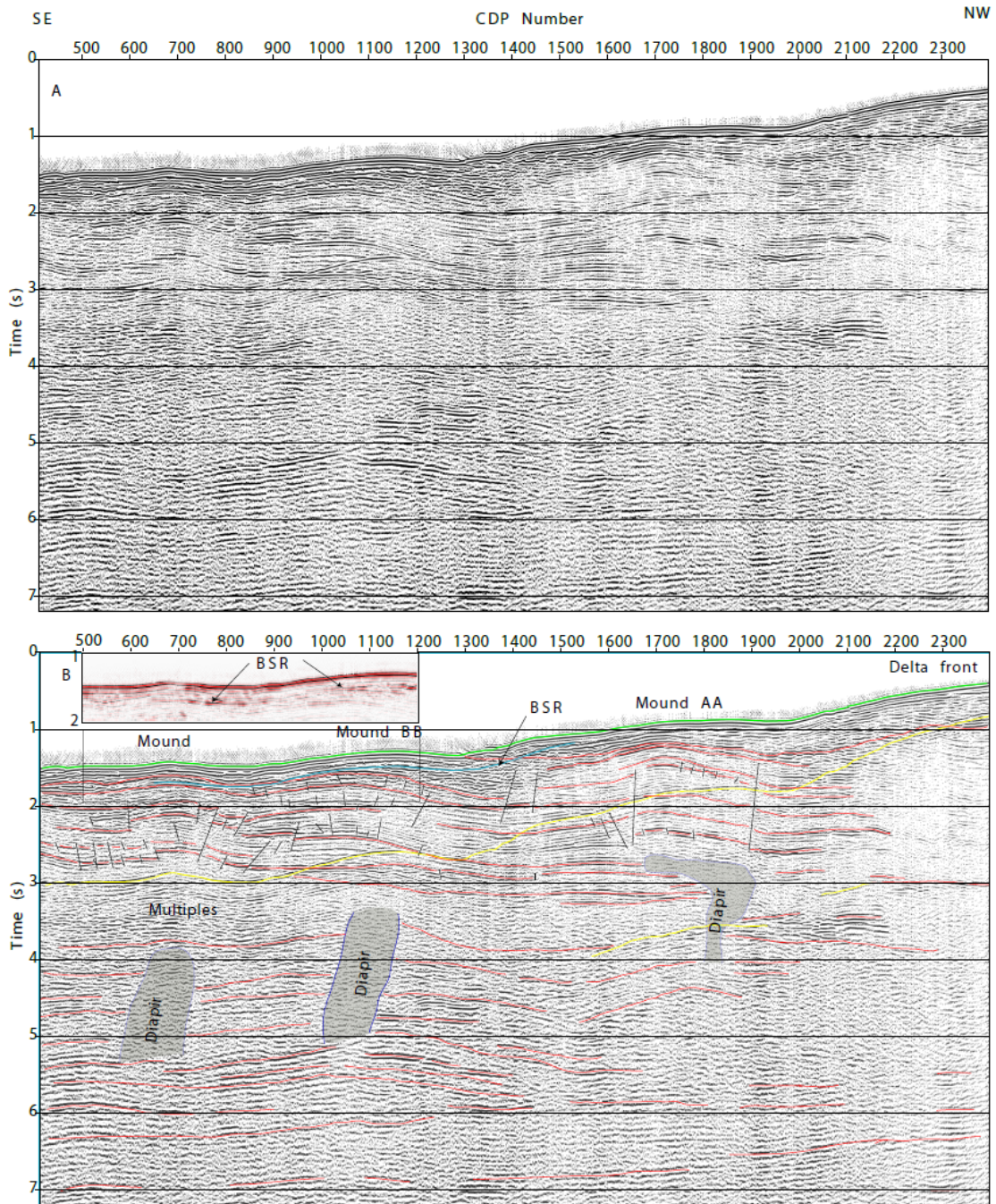


Figure 9

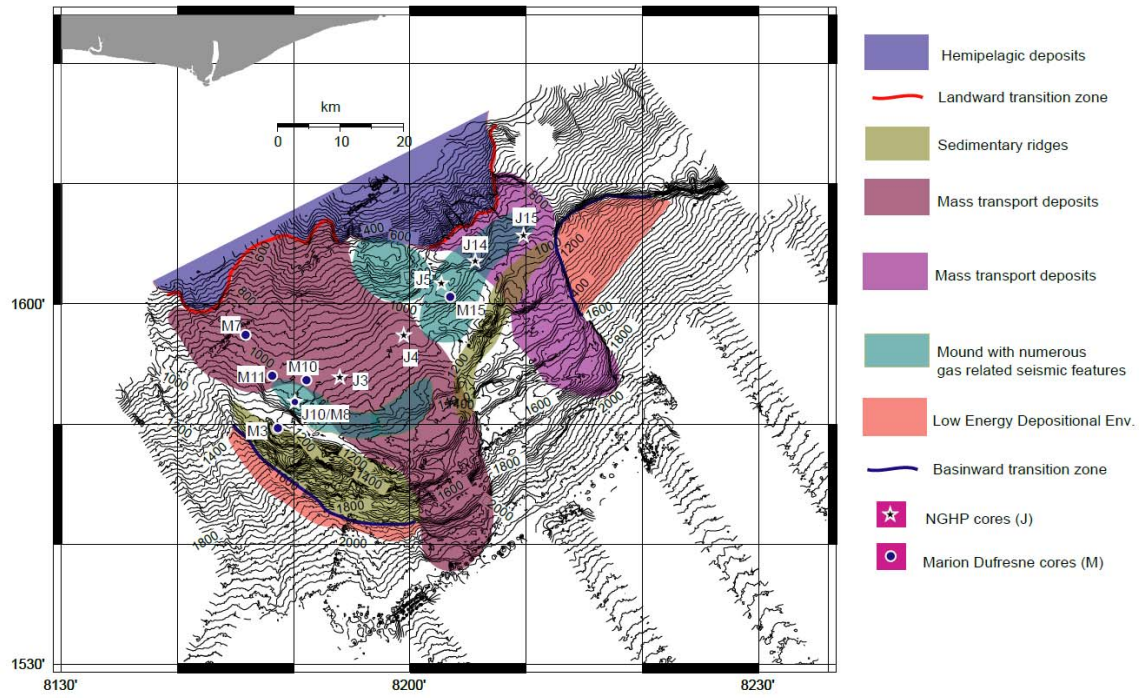


Figure 10

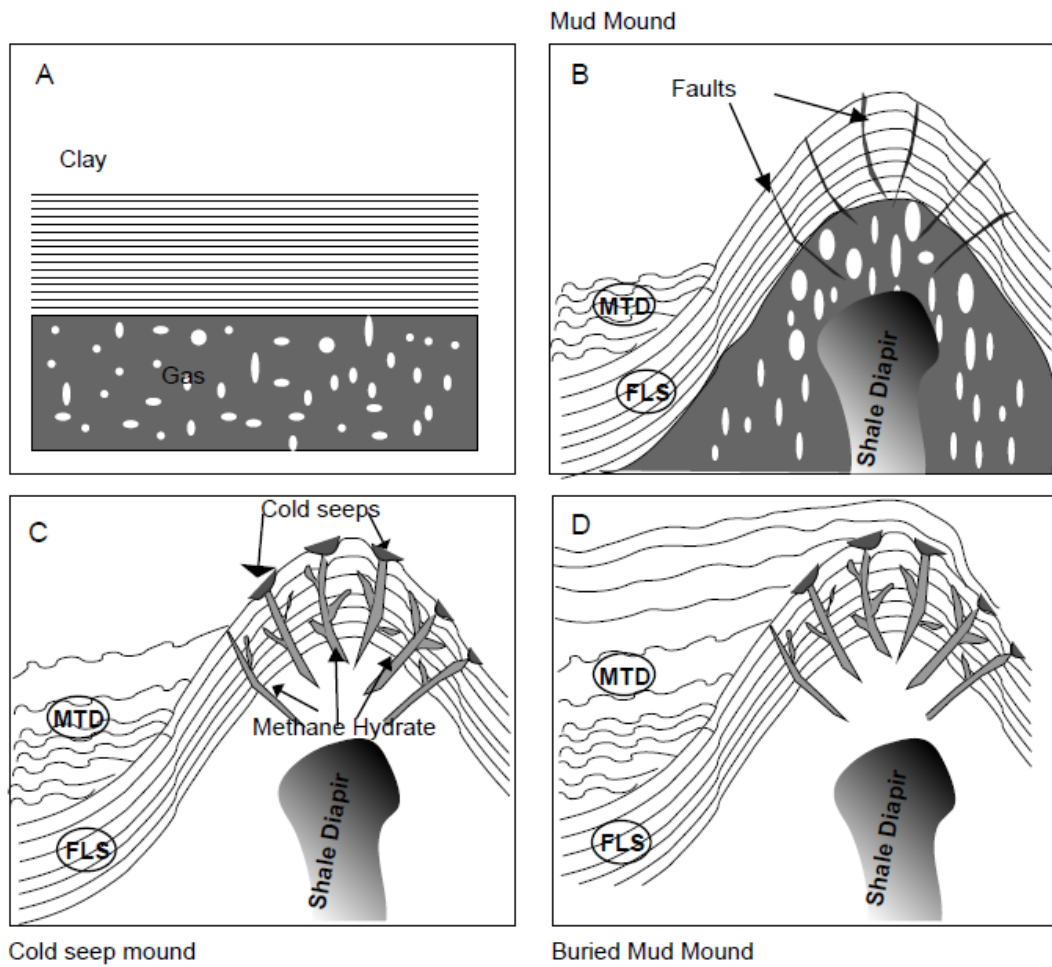


Figure 11

Datasets	Coverage of data during different cruises in KG offshore basin			Source
	R/V Sagar Kanya (SK-176)	R/V Sagar Nidhi (SN21)	R/V Marion Dufresne (MD161)	
Bathymetry	~3400 sq. km	---	~1630 sq. km	NIO*
High resolution Sparker data	---	~1250 lkm	---	NIO*
SBP	---	~2350 lkm	~1000 lkm	NIO*

* NIO – National Institute of Oceanography, Goa, India

Table 1